Computer Assisted Mechanics and Engineering Sciences, 9: 543–553, 2002.

A variant of the method of characteristics[1]

Mario Šavar and Zdravko Virag
University of Zagreb, Faculty of Mechanical Engineering and Naval Architecture
I. Lučića 5, 10000 Zagreb, Croatia

Radoslav Korbar
Polytechnics of Karlovac, Department of Mechanical Engineering
I. Meštrovića 10, 47000 Karlovac, Croatia

(Received February 9, 2001)

A variant of the method of characteristics for hyperbolic conservation laws is proposed in this paper. It is based on the time interpolation instead of space interpolation as in the standard method of characteristics. A new method for calculating the propagation velocity is proposed as well. The numerical results of some presented typical tests indicate that algorithm is very accurate.

1. Introduction

A new interpolation scheme for hyperbolic conservation laws is proposed in this paper. It is based on the method of characteristics, which is very popular for solving many engineering problems such as pressure transients in pipelines, dynamics of gas networks, water hammer, flow in open channels and many others.

The main reason for introducing the new scheme is the reduction in the numerical diffusion error. The proposed scheme is based on time interpolation (as described in Section 2) instead of the usual practice that employs space interpolation in the method of characteristics. A new method for calculating the propagation velocity is proposed in this paper, as well. In Section 3, the proposed scheme is tested in some typical situations, such as the pure convection transport of passive scalar, the Burger's equation, the Sod problem and the simple water hammer problem. The applicability and advantages of the proposed scheme are presented in Section 4.

2. Description of the scheme

A large number of physical systems may be entirely or partially described by the following partial differential equation,

$$\frac{\partial U}{\partial t} + \frac{\partial F}{\partial x} = Q, \tag{1}$$

where U represents the vector of unknowns, function $F(U)$ is the flux vector and Q is the source term vector. In the context of fluid dynamics, Eq. (1) may describe a number of actual technical problems.

There is a certain class of problems in which the source term Q contains second order derivatives of unknowns U. If the magnitude of terms on the left-hand side dominate over the source term,

[1]This is an extended version of the article presented at the 8th International Conference on Numerical Methods in Continuum Mechanics, Liptovský Ján, Low Tatras, Slovakia, September 19–24, 2000.

system (1) may be numerically treated as a set of hyperbolic differential equations. It can be rewritten as follows,

$$\frac{\partial U}{\partial t} + A\frac{\partial U}{\partial x} = Q, \tag{2}$$

where A is the Jacobian defined by $A = \frac{\partial F}{\partial U}$. Every set of hyperbolic differential equations may be represented in the characteristic form [2]

$$\frac{\partial W}{\partial t} + \Lambda\frac{\partial W}{\partial x} = B, \tag{3}$$

where W is the vector of characteristic variables, Λ is the diagonal matrix containing the propagation velocities of characteristic variables and B is the vector of source terms. Every equation of the system (3) may be considered independently and written in the form

$$\frac{D_i w_i}{Dt} \equiv \frac{\partial w_i}{\partial t} + \lambda_i\frac{\partial w_i}{\partial x} = b_i\,, \tag{4}$$

where w_i and b_i represent the i-th components of vectors W and B, respectively, while λ_i is the corresponding diagonal term of the matrix Λ. Equation (4) is valid along the characteristic line C_i defined by the equation

$$\frac{\mathrm{d}x}{\mathrm{d}t} = \lambda_i\,.$$

2.1. The method of characteristics

The variation of the variable $w_i = w$ along the characteristic $C_i = C$ depends only on the source term $b_i = b$. For $\lambda = \text{const}$, the characteristic line is a straight line as shown in Fig. 1. For the time-space grid defined in Fig. 1, Eq. (4) can be approximated by the following algebraic equation [1],

$$w_i^{n+1} - w^0 = b\Delta t. \tag{5}$$

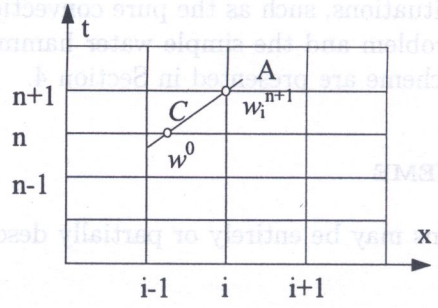

Fig. 1. Characteristic line C and the definition of time-space grid

The value $w_0$can be calculated by linear interpolation from the values of the variable w at nodes $(i-1, n)$ and (i, n),

$$w^0 = CFL \cdot w_{i+1}^n + (1 - CFL) \cdot w_i^n\,, \tag{6}$$

where CFL is the Courant–Friedrichs–Levy number $CFL = \lambda\Delta t/\Delta x$, Δt is the integration time step and Δx is the integration space step. The method of characteristics is stable for $CFL \leq 1$.

2.2. The proposed variant of the method of characteristics

The analysis of the diffusion error of the standard method of characteristics shows that the essential part of the error is made by interpolation (6). In order to reduce the interpolation error, a new interpolation scheme is suggested.

The new scheme proposes the time interpolation at a fixed space node (e.g. w_0 is calculated by linear interpolation from the values of the variable w at nodes $(i-1, n-1)$ and $(i-1, n-2)$ as shown in Fig. 2) instead of the space interpolation at a fixed time (as shown in Fig. 1).

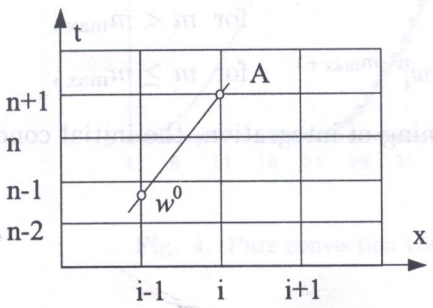

Fig. 2. Proposed interpolation scheme

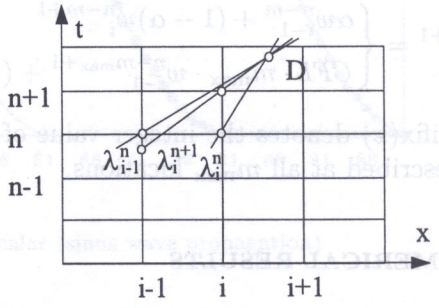

Fig. 3. Interpolation of characteristic line

At low *CFL* numbers, the standard method of characteristics generates a considerable numeric diffusion error. In the proposed scheme, the values at the appropriate two previous time nodes are used for the interpolation, which generates a smaller diffusion error. The fact that values of numerous time steps must be memorized for a single space step presents the major drawback of the method. In the extreme case, when *CFL* number equals zero, an infinite number of time steps should be memorized.

Because of memory limitations, the fixed number $m_{\max}$ of time steps is memorized, and the new interpolation scheme is applied only if $1/CFL \leq m_{\max}$. In the other case, the standard method of characteristics is applied (but interpolating in the $(n - m_{\max} + 1)\Delta t$ period of time).

A precise approximation of the propagation velocity λ is important for the accuracy of the interpolation scheme. All nodes lie in the compression (as shown in Fig. 3) or expansion wave zone (except for the trivial solution when the propagation velocity is constant). The propagation velocity is calculated from the condition that all waves reach the point D at the same time and form a shock wave (all characteristics will intersect at the point D as shown in Fig. 3). The propagation velocity is given by the following expression (valid for the expansion and compression wave alike),

$$\lambda = \frac{\lambda_i^n}{1 + \frac{\Delta t}{\Delta x}(\lambda_i^n - \lambda_{i-1}^n)}. \tag{7}$$

When the shock wave is formed within the interval between the nodes $(i-1, n)$ and (i, n), the propagation velocity is calculated by [4]

$$\lambda = \frac{\lambda_{i-1}^n + \lambda_i^n}{2}. \tag{8}$$

The proposed interpolation scheme is completely described by the following equations for $\lambda_{i-1} > 0$,

$$\lambda = \begin{cases} \dfrac{\lambda_i^n}{1 + \frac{\Delta t}{\Delta x}(\lambda_i^n - \lambda_{i-1}^n)} & \text{for } \dfrac{\lambda_i^n}{\lambda_{i-1}^n} > 0, \\ \dfrac{\lambda_i^n + \lambda_{i-1}^n}{2} & \text{for } \dfrac{\lambda_i^n}{\lambda_{i-1}^n} \le 0, \end{cases}$$

$$CFL = \frac{\lambda \Delta x}{\Delta x}, \qquad m = \mathrm{ifix}\left(\frac{1}{CFL}\right), \qquad \alpha = \frac{1}{CFL} - m, \tag{9}$$

$$w_i^{n+1} = \begin{cases} \alpha w_{i-1}^{n-m} + (1-\alpha) w_i^{n-m+1} & \text{for } m < m_{\max}, \\ CFL \cdot m_{\max} \cdot w_{i-1}^{n-m_{\max}+1} + (1 - CFL \cdot m_{\max}) w_i^{n-m_{\max}+1} & \text{for } m \ge m_{\max}, \end{cases}$$

where $\mathrm{ifix}(x)$ denotes the integer value of x. At the beginning of integration, the initial conditions are prescribed at all $m_{\max}$ locations.

3. Numerical results

In this section, numerical results of several tests are given to show the capability of the new interpolation scheme.

3.1. Pure convection transport of passive scalar

The first test situation for the proposed interpolation scheme was the pure convection of passive scalar with a steady boundary condition and a smooth initial condition. The corresponding transport equation is

$$\Lambda = v, \qquad B = 0, \tag{10}$$

where v is the fluid velocity. Equation (3) becomes

$$\frac{\partial w}{\partial t} + v \frac{\partial w}{\partial x} = 0 \tag{11}$$

while the initial condition is given by the expressions

$$\begin{aligned} w(x,0) &= 0.5 + 0.5 \sin\left(\frac{x-2}{60} 2\pi - \frac{\pi}{2}\right) && \text{for } 2 < x < 62, \\ w(x,0) &= 0 && \text{for } x \ge 62. \end{aligned} \tag{12}$$

It is known that for this case the numerical results of the method of characteristics, when integrated at $CFL = 1$, completely agree with the exact solution. Here the integration was performed on 100 equally spaced mesh points within the interval [1,101], with $v = 1$ and $CFL = 0.9$. (The same integration parameters in the same domain were used also for the next test case). The numerical results after 22 and 44 time steps are presented in Fig. 4. The numerical results are presented by discrete points, and the exact solution by the solid line (in other figures, the same designation is applied). Excellent agreement of numerical results with the exact solution was achieved.

The test with discontinuous initial conditions is a rather demanding one. The goal is to reproduce the discontinuity as accurate as possible (position, shape and amplitude). The same transport equation (11) was tested with the discontinuous initial conditions given by the equation

$$\begin{aligned} w(x,0) &= 1 \quad \text{for } 1 < x < 51, \\ w(x,0) &= 0 \quad \text{for } x = 1 \text{ and } x > 50. \end{aligned} \tag{13}$$

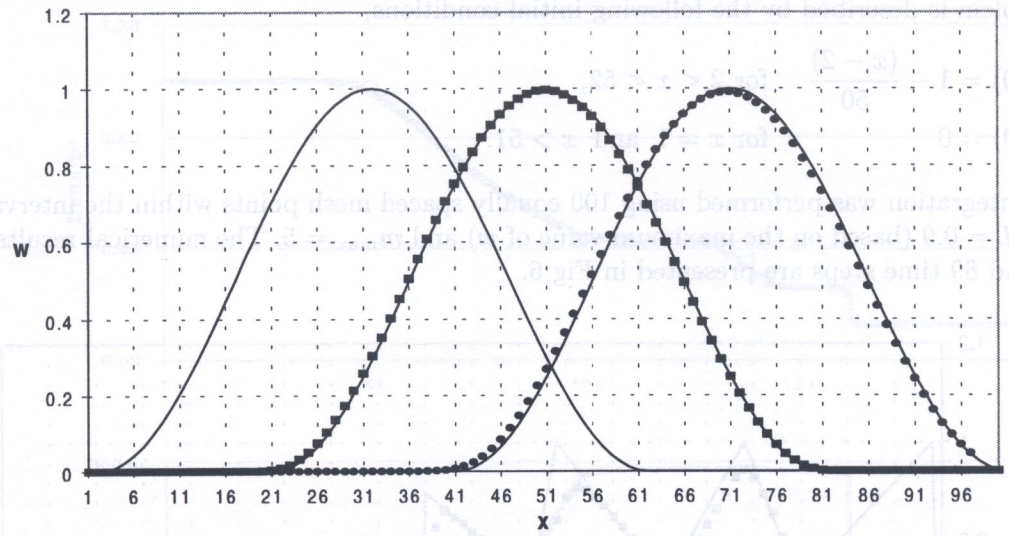

Fig. 4. Pure convection transport of passive scalar (sinus wave propagation)

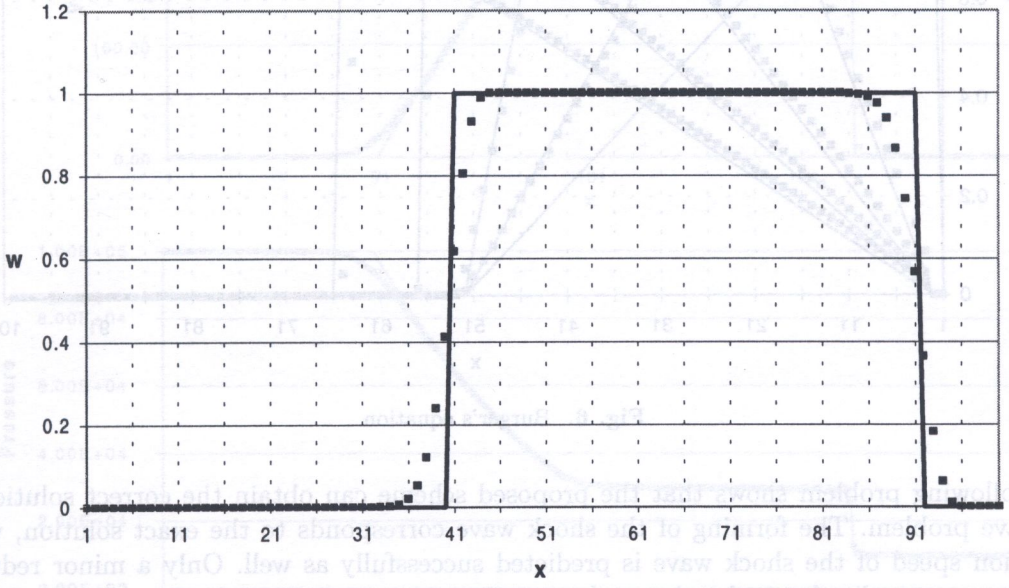

Fig. 5. Pure convection transport of passive scalar (propagation of step)

The numerical result after 44 time steps is presented in Fig 5.

From the numerical results, it is obvious that the scheme predicts the position of the discontinuities accurately, only with a minor numerical diffusion error. The shape of the step function is preserved. It can also be observed that non-physical oscillations, which often accompany high order schemes, did not occur here.

3.2. Shock wave problem (Burger's equation)

The simplest and the most frequent test for inviscid non-linear flow problems is the Burger's equation,

$$\Lambda = w, \qquad B = 0, \qquad \frac{\partial w}{\partial t} + w \frac{\partial w}{\partial x} = 0. \tag{14}$$

The problem is described by the following initial conditions,

$$\begin{aligned} w(x,0) &= 1 - \frac{(x-2)}{50} \quad \text{for } 2 < x < 52, \\ w(x,0) &= 0 \qquad\qquad\quad \text{for } x = 1 \text{ and } x > 51. \end{aligned} \tag{15}$$

The integration was performed using 100 equally spaced mesh points within the interval [1,101], with $CFL = 0.9$ (based on the maximum value of w) and $m_{\max} = 5$. The numerical results after 22, 44, 67 and 89 time steps are presented in Fig 6.

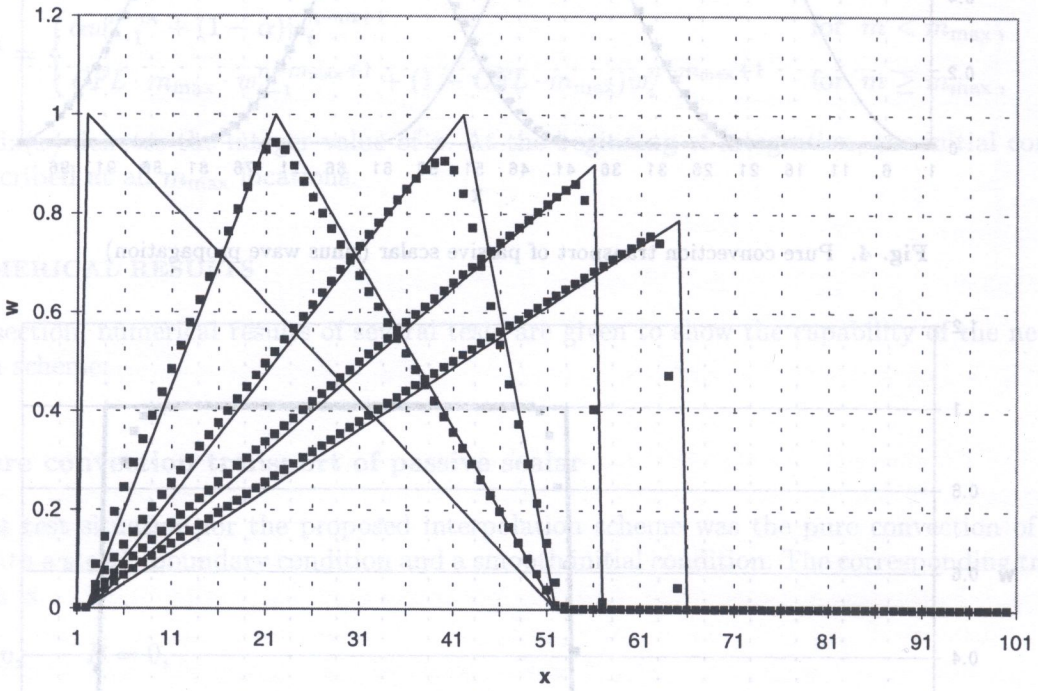

Fig. 6. Burger's equation

The following problem shows that the proposed scheme can obtain the correct solution to the shock wave problem. The forming of the shock wave corresponds to the exact solution, while the propagation speed of the shock wave is predicted successfully as well. Only a minor reduction in the shock wave amplitude can be observed.

3.3. Shock wave tube problem (Sod's test problem)

The most popular test for compressible inviscid fluid flow is the Sod's shock wave tube problem [3]. The fluid flow model is presented by the Euler's equations of gas dynamics,

$$\frac{\partial U}{\partial t} + \frac{\partial F}{\partial x} = 0, \qquad U = \begin{pmatrix} \rho \\ \rho v \\ \rho e \end{pmatrix}, \qquad F = \begin{pmatrix} \rho v \\ \rho v^2 + p \\ v(p + \rho e) \end{pmatrix}, \tag{16}$$

where v, ρ, p, e are the fluid velocity, density, pressure and the total energy of gas per unit mass, respectively. The characteristic forms of Eqs. (16) are

$$\frac{Dw_1}{Dt} = 0, \qquad \frac{D^+ w_2}{Dt} = 0, \qquad \frac{D^- w_3}{Dt} = 0, \tag{17}$$

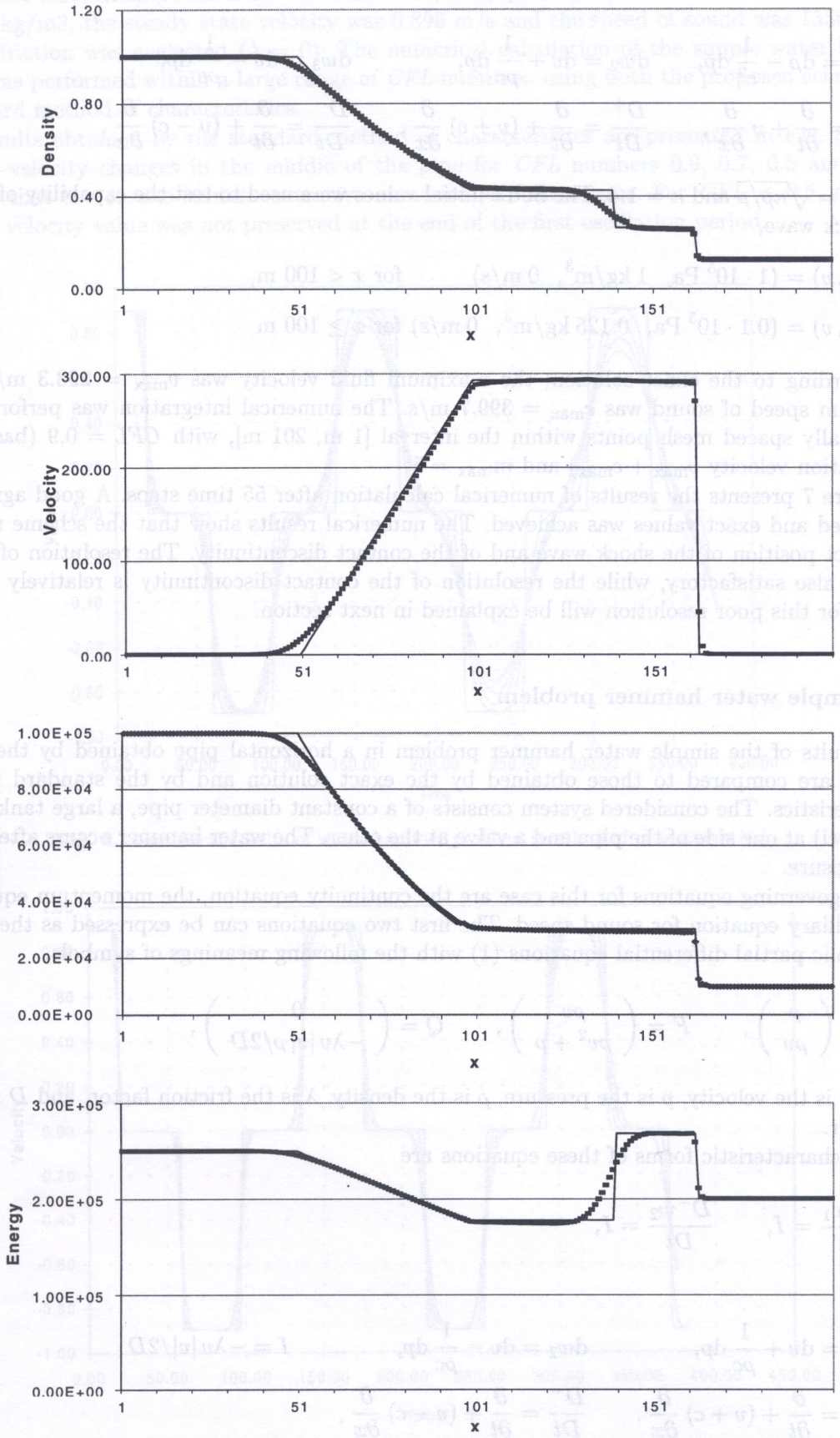

Fig. 7. Numerical results of the shock tube problem

where

$$\begin{aligned} &dw_1 = d\rho - \frac{1}{c^2}\,dp, \qquad dw_2 = dv + \frac{1}{\rho c}\,dp, \qquad dw_3 = dv - \frac{1}{\rho c}\,dp, \\ &\frac{D}{Dt} = \frac{\partial}{\partial t} + v\,\frac{\partial}{\partial x}, \qquad \frac{D^+}{Dt} = \frac{\partial}{\partial t} + (v+c)\,\frac{\partial}{\partial x}, \qquad \frac{D^-}{Dt} = \frac{\partial}{\partial t} + (v-c)\,\frac{\partial}{\partial x}, \end{aligned} \tag{18}$$

where $c = \sqrt{\kappa p/\rho}$ and $\kappa = 1.4$. The Sod's initial values were used to test the capability of capturing the shock wave,

$$\begin{aligned} &(p, \rho, v) = (1 \cdot 10^5\ \text{Pa},\ 1\ \text{kg/m}^3,\ 0\ \text{m/s}) \qquad \text{for } x < 100\ \text{m}, \\ &(p, \rho, v) = (0.1 \cdot 10^5\ \text{Pa},\ 0.125\ \text{kg/m}^3,\ 0\ \text{m/s}) \quad \text{for } x \geq 100\ \text{m}. \end{aligned} \tag{19}$$

According to the exact solution, the maximum fluid velocity was $v_{\max} = 293.3$ m/s and the maximum speed of sound was $c_{\max} = 399.7$ m/s. The numerical integration was performed using 200 equally spaced mesh points within the interval [1 m, 201 m], with $CFL = 0.9$ (based on the propagation velocity $v_{\max} + c_{\max}$) and $m_{\max} = 5$.

Figure 7 presents the results of numerical calculation after 55 time steps. A good agreement of calculated and exact values was achieved. The numerical results show that the scheme reproduces the exact position of the shock wave and of the contact discontinuity. The resolution of the shock wave is also satisfactory, while the resolution of the contact discontinuity is relatively poor. The reason for this poor resolution will be explained in next section.

3.4. Simple water hammer problem

The results of the simple water hammer problem in a horizontal pipe obtained by the proposed method are compared to those obtained by the exact solution and by the standard method of characteristics. The considered system consists of a constant diameter pipe, a large tank (constant fluid level) at one side of the pipe and a valve at the other. The water hammer occurs after a sudden valve closure.

The governing equations for this case are the continuity equation, the momentum equation and the auxiliary equation for sound speed. The first two equations can be expressed as the system of hyperbolic partial differential equations (1) with the following meanings of symbols,

$$U = \begin{pmatrix} \rho \\ \rho v \end{pmatrix}, \qquad F = \begin{pmatrix} \rho v \\ \rho v^2 + p \end{pmatrix}, \qquad Q = \begin{pmatrix} 0 \\ -\lambda v\,|v|\,\rho/2D \end{pmatrix}, \tag{20}$$

where v is the velocity, p is the pressure, ρ is the density, λ is the friction factor, and D is the pipe diameter.

The characteristic forms of these equations are

$$\frac{D^+ w_1}{Dt} = I, \qquad \frac{D^- w_2}{Dt} = I, \tag{21}$$

where

$$\begin{aligned} &dw_1 = dv + \frac{1}{\rho c}\,dp, \qquad dw_2 = dv - \frac{1}{\rho c}\,dp, \qquad I = -\lambda v\,|v|/2D \\ &\frac{D^+}{Dt} = \frac{\partial}{\partial t} + (v+c)\,\frac{\partial}{\partial x}, \qquad \frac{D^-}{Dt} = \frac{\partial}{\partial t} + (v-c)\,\frac{\partial}{\partial x}, \end{aligned} \tag{22}$$

where c is the constant speed of sound.

In the test case, the pipe diameter was 10.97 mm, the pipe length was 91.41 m, the fluid density was 992.8 kg/m3, the steady state velocity was 0.896 m/s and the speed of sound was 1336.5 m/s, while the friction was neglected ($\lambda = 0$). The numerical calculation of the simple water hammer problem was performed within a large range of *CFL* numbers, using both the proposed scheme and the standard method of characteristics.

The results obtained by the standard method of characteristics are presented in Fig. 8, which shows the velocity changes in the middle of the pipe for *CFL* numbers 0.9, 0.7, 0.5 and 0.3. It is obvious that the results contain extensive numerical diffusion error. For $CFL < 0.5$, even the maximum velocity value was not preserved at the end of the first oscillation period.

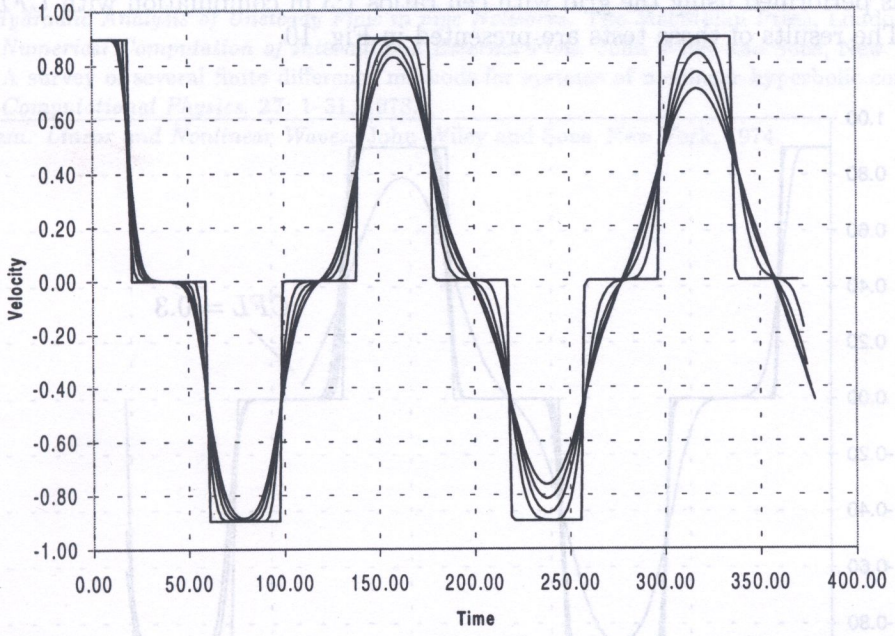

Fig. 8. Numerical results of water hammer problem (method of characteristics)

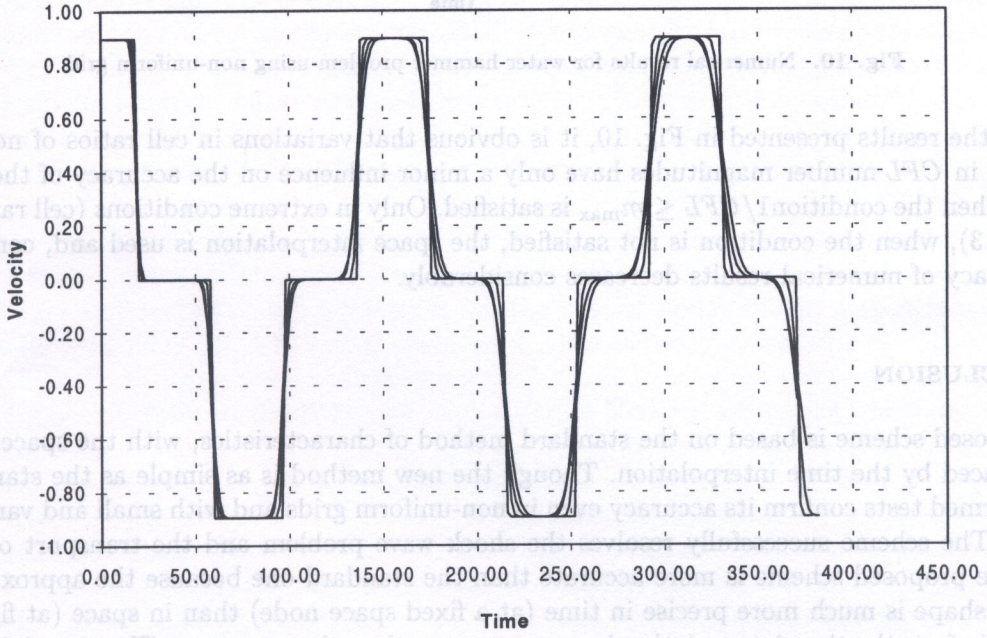

Fig. 9. Numerical results of water hammer problem (proposed method)

The numerical results obtained by the proposed method with $m_{\max} = 5$ are presented in Fig. 9 for the same velocity changes and *CFL* numbers shown in Fig. 8.

The comparison of results in Figs. 8 and 9 shows that the new scheme produces significantly smaller numerical diffusion error. Therefore its superiority over the standard method of characteristics is beyond doubt. However, the proposed method imposes the requirement $1/CFL \leq m_{\max}$, which guarantees a relatively small numerical diffusion error. If this condition is not satisfied, the proposed method generates solutions similar to those obtained by the standard method of characteristic. To illustrate this behavior, the following test was performed. The numerical integration was performed by the proposed scheme using two non-uniform grids with length ratios of two neighboring cells 1:2 and 2:1. These grids were combined with *CFL* numbers 0.9, 0.7, 0.5 and 0.3. The same procedure was performed using the grid with cell ratios 1:3 in combination with *CFL* numbers 0.9, 0.7 and 0.3. The results of these tests are presented in Fig. 10.

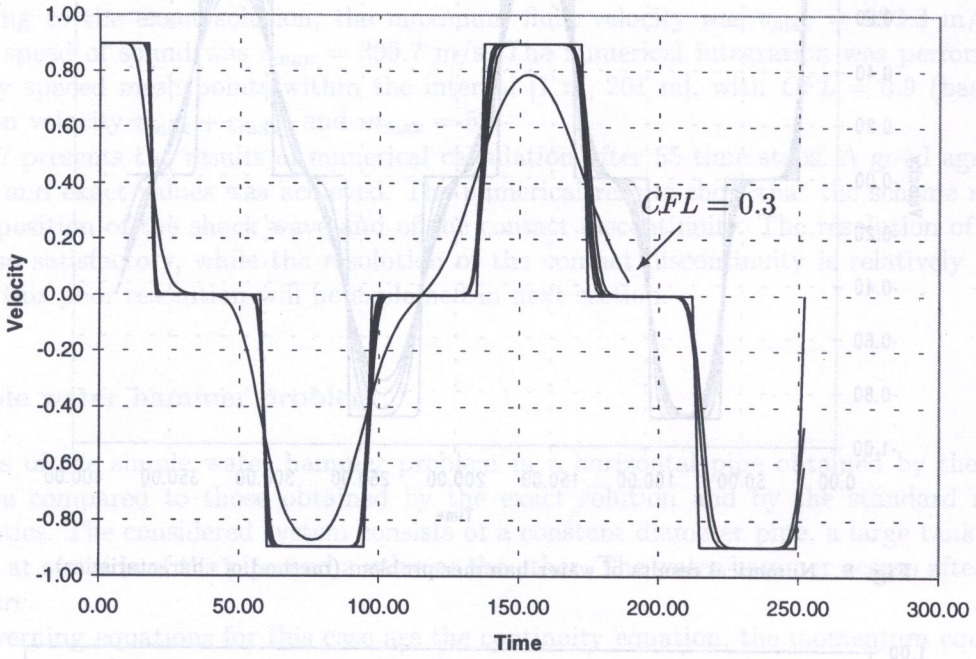

Fig. 10. Numerical results for water hammer problem using non-uniform grid

From the results presented in Fig. 10, it is obvious that variations in cell ratios of non-uniform grids and in *CFL* number magnitudes have only a minor influence on the accuracy of the proposed scheme when the condition$1/CFL \leq m_{\max}$ is satisfied. Only in extreme conditions (cell ratio 1:3 and $CFL = 0.3$), when the condition is not satisfied, the space interpolation is used and, consequently, the accuracy of numerical results decreases considerably.

4. Conclusion

The proposed scheme is based on the standard method of characteristics, with the space interpolation replaced by the time interpolation. Though the new method is as simple as the standard one, the performed tests confirm its accuracy even in non-uniform grids and with small and variable *CFL* number. The scheme successfully resolves the shock wave problem and the transport of discontinuity. The proposed scheme is more accurate than the standard one because the approximation of the wave shape is much more precise in time (at a fixed space node) than in space (at fixed time). Due to this fact, the time interpolation is more accurate than the space one. That is valid especially for non-uniform grids and small *CFL* numbers. The accuracy of the new scheme decreases when

the condition $1/CFL \leq m_{\max}$ is not satisfied because this leads to a space interpolation similar to the one in the standard method of characteristics. In that case, the accuracy can be recovered by increasing the parameter $m_{\max}$. The necessity of memorizing $m_{\max}$ previous time steps presents the main disadvantage of the method and imposes a great barrier to its applicability in multidimensional cases.

In order to improve the solution accuracy, the proposed scheme can be easily incorporated in existing codes (based on the method of characteristics) for solving water hammer problems.

References

[1] J.A. Fox. *Hydraulic Analysis of Unsteady Flow in pipe Networks.* The MacMillan Press, London, 1997.

[2] C. Hirsch. *Numerical Computation of Internal and External Flow.* John Wiley and Sons, New York, 1990.

[3] G.A. Sod. A survey of several finite difference methods for systems of nonlinear hyperbolic conservation laws. *Journal of Computational Physics*, **27**: 1–31, 1978.

[4] G.B. Whitam. *Linear and Nonlinear Waves.* John Wiley and Sons, New York, 1974.